PAPER

Forward bias annealing of proton radiation damage in NiO/Ga_2O_3 rectifiers

To cite this article: Jian-Sian Li *et al* 2024 *Phys. Scr.* **99** 075312

Physica Scripta

PAPER

Forward bias annealing of proton radiation damage in NiO/Ga_2O_3 rectifiers

RECEIVED
27 February 2024

REVISED
19 May 2024

ACCEPTED FOR PUBLICATION
6 June 2024

PUBLISHED
20 June 2024

Jian-Sian Li[1], Chao-Ching Chiang[1], Hsiao-Hsuan Wan[1], Md Abu Jafar Rasel[2], Aman Haque[2], Jihyun Kim[3], Fan Ren[1], Leonid Chernyak[4] and S J Pearton[5]

[1] Department of Chemical Engineering, University of Florida, Gainesville, FL 32611, United States of America
[2] Mechanical Engineering, The Pennsylvania State University, University Park, PA 16802, United States of America
[3] Department of Chemical and Biological Engineering, Seoul National University, Seoul 08826, Republic of Korea
[4] Departmen of Physics, University of Central Florida, Orlando, FL 32816, United States of America
[5] Department of Materials Science and Engineering, University of Florida, Gainesville, FL 32611, United States of America

E-mail: jiansianli@ufl.edu

Keywords: gallium oxide, nickel oxide, rectifiers, proton irradiation

Abstract

17 MeV proton irradiation at fluences from 3–7 $\times 10^{13}$ cm^{-2} of vertical geometry NiO/β-Ga_2O_3 heterojunction rectifiers produced carrier removal rates in the range 120–150 cm^{-1} in the drift region. The forward current density decreased by up to 2 orders of magnitude for the highest fluence, while the reverse leakage current increased by a factor of ~20. Low-temperature annealing methods are of interest for mitigating radiation damage in such devices where thermal annealing is not feasible at the temperatures needed to remove defects. While thermal annealing has previously been shown to produce a limited recovery of the damage under these conditions, athermal annealing by minority carrier injection from NiO into the Ga_2O_3 has not previously been attempted. Forward bias annealing produced an increase in forward current and a partial recovery of the proton-induced damage. Since the minority carrier diffusion length is 150–200 nm in proton irradiated Ga_2O_3, recombination-enhanced annealing of point defects cannot be the mechanism for this recovery, and we suggest that electron wind force annealing occurs.

Introduction

Monoclinic β-Ga_2O_3 has recently garnered significant attention for power switching devices and solar-blind UV photodetectors [1–14]. Notable advancements have been made in NiO/β-Ga_2O_3 power rectifiers, surpassing the performance of GaN [15–25]. Experimental investigations have revealed maximum breakdown voltages above 8 kV, corresponding to critical electric fields $>$ 8 MV cm^{-1} [23–25]. The intended applications for Ga_2O_3 power electronics include next-generation power, GHz switching and RF applications, including the traction inverter, dc-dc converter and on-board charger for electric vehicles, as well as distributed energy resource systems and uni- and bi-directional power converters for renewable energy systems [2, 6, 8, 13].

The lack of p-type doping for Ga_2O_3 initially limited power devices to unipolar Schottky Barrier Diode (SBD) and Metal Oxide Semiconductor Field Effect Transistors (MOSFETs) [2, 5]. However, the implementation of p-type NiO to form heterojunctions with n-type Ga_2O_3 has led to demonstrations of vertical rectifiers with excellent high-temperature operation [15–25]. The wide bandgap of Ga_2O_3 means less charge is deposited during radiation exposure than for narrower gap materials and combined with the higher bond strength and high rate of dynamic annealing, indicates that Ga_2O_3 may be well-suited to high radiation environments [26–31]. Ga_2O_3 demonstrates notable resilience against total ionizing dose (TID) effects [27, 28]. Recent investigations have reported single-event burnout (SEB) in Ga_2O_3 rectifiers [32, 33]. Strategies involving field management have been proposed to partially mitigate single-event effects[32–35].

The minimization of displacement damage in semiconductors is key to enhancing their survivability in environments where they are subject to high fluences of ionizing particles, such as satellites, defense systems and nuclear reactor control electronics. While shielding or turning off the devices if it is known that a radiation event

will occur are some of the methods employed for reducing the effects of radiation damage, at a device level, various types of annealing may be possible. For example, in similar NiO/Ga_2O_3 rectifiers to those studied here, annealing at 400 °C was partially successful in restoring the initial properties [36]. While the reverse leakage increased due to reaction of the contacts, the forward current and the initial carrier density in the drift region were significantly restored by this thermal annealing [36].

There are three basic carrier-driven mechanisms known to produce near-athermal annealing of defects in semiconductors. Firstly, Recombination Enhanced Defect Reactions (REDR) involve vibrational energy locally deposited at defects by nonradiative electronic transitions [37, 38]. This additional energy will increase defect annealing or reaction rates [38]. This mechanism requires a pn junction and a large enough minority carrier diffusion length to affect traps within a device structure. This has been shown to cause recombination-enhanced annealing of point defects in numerous semiconductors [37–45]. Recombination-enhanced annealing of defects is well-established in Ga_2O_3, with both optical and electrical injection of minority carriers leading to increased carrier diffusion length and lifetime. Chernyak *et al* [39–45] have shown the transport properties of many other semiconductors, including ZnO and GaN, can be improved by minority carrier injection, attributed to increased minority carrier lifetime due to trapping of carriers on native point defects.

Secondly, during ion irradiation, there can be ionization enhanced-energy transfer from ions to binding electrons in the atomic structure via electron–phonon coupling [46, 47]. This electronic energy transfer can also lead to annealing of damage and is reported in many semiconductor systems [46, 47]. For example, in Ga_2O_3, Azarov *et al* [48] have shown that implanting ions at 300 °C effectively suppresses the defect formation. By sharp contrast, in order to reach similar crystalline quality in the samples implanted at room temperature, post-irradiation anneals in excess of 900 °C are necessary. It plays a role in the so-called dynamic annealing that is significant in Ga_2O_3 [27, 48].

Thirdly, Electron Wind Force (EWF) annealing occurs by electron momentum transfer to enhance defect annealing kinetics [49–60]. The mechanical force originates from the use of a high current density at a low duty cycle to suppress heat accumulation. Rasel *et al* [49] demonstrated that short, high current density pulses can mobilize and anneal defects produced by ^{60}Co gamma irradiated of GaN high electron mobility transistors, as well as existing defects in SiC Schottky barrier diodes [52]. The EWF mechanism is well-established in electromigration and electroplasticity studies [55–60], but its application to annealing defects in electronic devices can potentially be a powerful method to reverse the degradation of devices. It is generally accepted that the athermal impact of electromigration, in addition to the thermal effect, causes the atomic diffusion to be accelerated by the electric current treatment [55–60]. Electric current can induce annealing in aluminum alloys, employing a mechanism that is not Joule heating [60].

In this paper, we report the effects of forward-biased carrier injection of carriers on damage created by 17 MeV protons in NiO/ β-Ga_2O_3 vertical rectifiers. The displacement damage from the protons reduces the carrier concentration in the drift region of the rectifiers and reduces forward current density [44]. Partial recovery of the proton-induced is observed by carrier injection.

Experimental

The vertical geometry rectifier structures were constructed with drift region that was 10 μm thick, grown by Hydride Vapor Phase Epitaxy. This was grown on a conducting Ga_2O_3 single crystal substrate [23–25]. The free carrier concentrstion in the drift region was 6.7×10^{15} cm^{-3}, while the substrate was heavily doped (10^{19} cm^{-3}) with a (001) surface orientation. To form the heterojunction, 20 nm of rf sputtered (13.56 MHz) NiO was then deposited at low power (70 W) and a working pressure of 3 mTorr from twin targets. The Ar/O_2 ratio was varied to produce p-typ doping in the range 10^{18}—2.6×10^{19} cm^{-3}. The device fbrication was concluded by depositing of Ti/Au on the back of the substrate and Ni/Au to the front surface where the NiO had been deposited. A schematic representation of the device structure is provided in figure 1. More details are given in reference [36].

The iiradiation with protons was carried out on a cyclotron at a fixed energy of 17 MeV and 10 nA beam current. The fluences were set at 3, 5 and 7×10^{13} cm^{-2} A. The theoretical ion profiles were obtained from the standard Stopping and Range of Ions in Matter (SRIM) code [61]. This showed the projected range of the 17 ,eV protons was ~760 μm (figure 2). This penetration depth is much larger than the substrate thickness. Therefore the protons create damage along their path through the NiO and the Ga_2O_3 drift region. The SR-NIEL simulator [62] was also used to estimate both the nuclear and electronic stopping energy losses. The non-ionizing energy, or nuclear stopping loss at this energy was calculated to be 5.7×10^{-3} MeV.cm^2 g^{-1}. By contrast, the electronic stopping energy loss was significantly higher at 18 MeV.cm^2 g^{-1} (figure 3). The latter represents energy loss due to ionization, which dissipates as heat and dies not induce lattice damage. The device DC characteristics were measured with an HP 4156 parameter analyzer, while capacitance–voltage measurements were conducted with

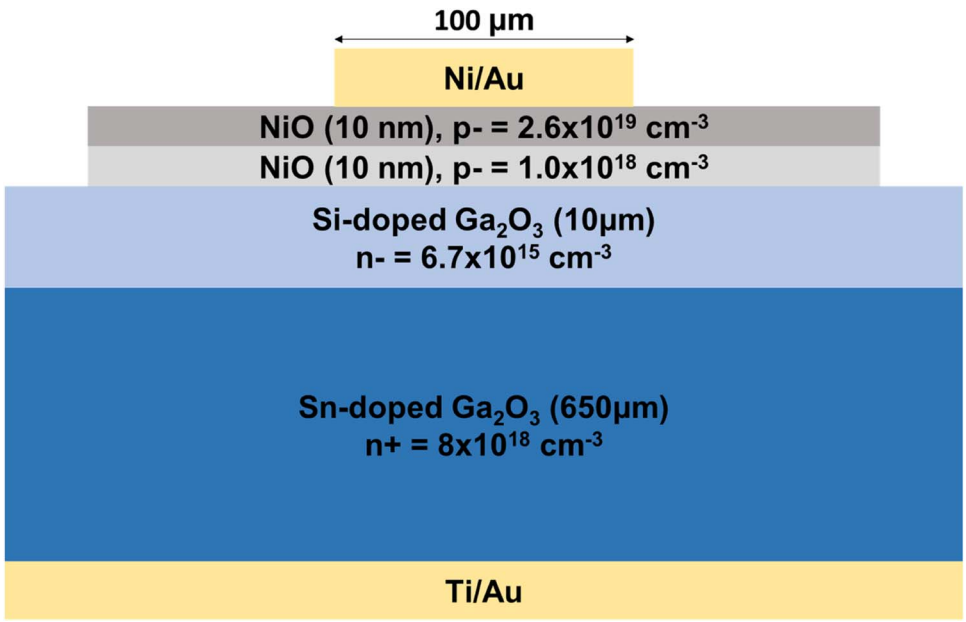

Figure 1. Schematic of the NiO/Ga_2O_3 HJD structure.

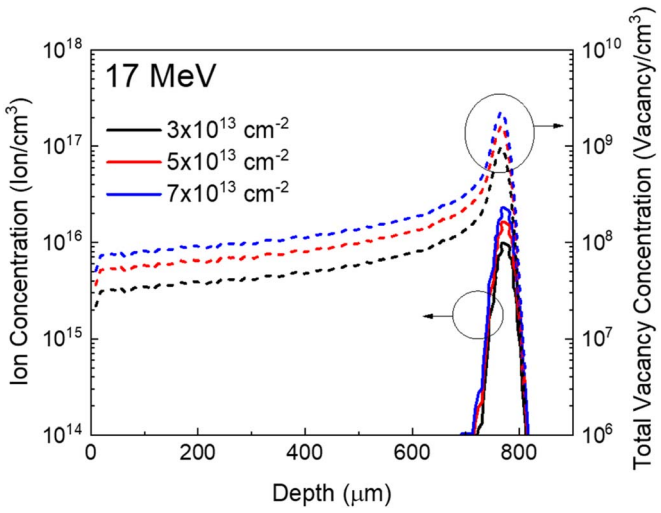

Figure 2. SRIM simulations of ion and damage profiles for 17 MeV H^+ implantation into NiO/Ga_2O_3 HJD structure. The damage peaks in the substrate, but a fairly constant profile of damage is created throughout the drift region.

an Agilent 4284 A Precision LCR Meter. Post-irradiation annealing was performed at 300 K by forward biasing at voltages ranging from 4–10 V for durations of 1–4 h.

Results and discussion

The first measurement was that of the forward current density–voltage (J-I) characteristics. The data from HJDs after irradiation at different fluences are illustrated in figure 4. The corresponding on-state resistance, R_{ON}, determined from the slope of these characteristics are also illustrated. Irradiation reduces this forward current density by up to two orders of magnitude. The current density is a function of both the carrier mobility and density. Therefore the creation of trapping states within the bandgap of the Ga_2O_3 reuduces the carrier concentration in the drift region and the intridction these scatring centrars also reudces the electron mobility. Both of thes effects lead to a smaller forward current. The R_{ON} of the rectifiers exhibit a corresponding two orders of magnitude increase at the 7×10^{13} cm^{-2} fluence. The linear plot in figure 4 elucidates the trends in forward current density with increasing fluence. As proton fluence rises, the slope of the J-V characteristics

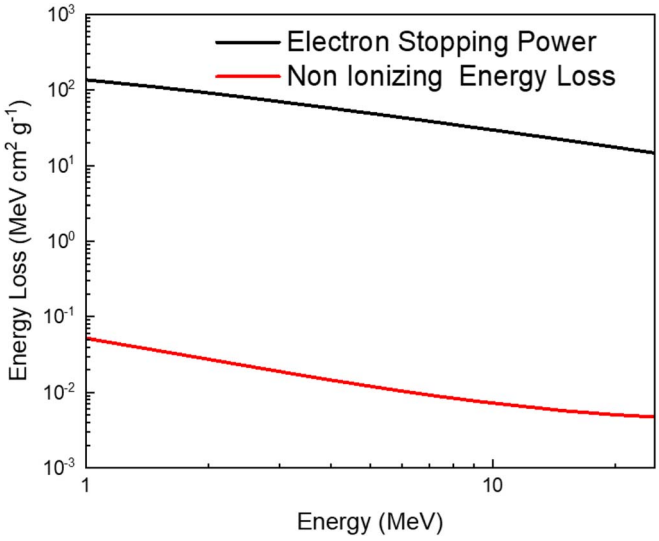

Figure 3. Electronic and -non-ionizing energy loss for protons in Ga_2O_3..

decreases, indicating an increase in R_{ON}. Additionally, the reverse current in the low bias voltage region as a function of fluence is presented in figure 4. The reverse current density increases by more than an order of magnitude due to the introduction of generation-recombination centers by proton damage. However, at the highest fluence, the current decreases again, as the competing mechanism of carrier loss to trap sites in the drift region becomes more significant.

The reduction in electron concentration in the lightly doped drift layer was determined from the C^{-2}-V characteristics, as depicted in figure 5 (top). The bottom portion of figure 5 presents the carrier distribution profiles obtained from the C-V data. This illustrates the higher rate of loss of carriers in the drift region for higher fluences. The carrier removal rates were found to be in the range of 120–150 cm^{-1} for the investigated fluence range. This aligns with studies for both NiO/Ga_2O_3 HJDs and Ni/ Ga_2O_3 Schottky diodes with the NiO layer [26, 27]. Figure 6 compiles the reported values for electron removal rate in Ga_2O_3 using protons of varying energies. The spread in literature values reflects the dependence of the carrier removal rate on the type of compensating impurities and pre-existing defects, as well as the startingelectron density in the drift region. At high fluences, the electron removal rate will saturate due to the fact all the carriers are trapped and additional introduction of defect states will not affect the electron density [36].

In order to study the effect of carrier injection on forward-biased devices, various bias levels and durations were tested. Recombination enhancement is a phenomenon where vibrational energy localized at a defect, and induced by a nonradiative electronic transition, accelerates the reaction rate. When the electronic energy fully transitions into vibrational excursions along the reaction pathway, the reaction rate is maximally augmented, corresponding to an effective reduction in barrier height—namely, the energy difference between the free and trapped electronic configurations.

Figure 7 shows improvements up to 20% in forward current density for biasing up to 10 V for a fixed duration of 30 min. These increases get larger with the magnituide of the applied bias voltage. For bias voltages beyond 10 V, an irreversible decrease in current density was evident, indicating potential degradation of device interfaces. Gong *et al* [63] reported that high carrie density injection conditions could lead to increased interface state densities at the top contact. The observed improvement in current density at moderate currents aligns with results reported by Rasel *et al* [49, 52]. That work invoked the electron wind force mechanism. The ame basic trends were observed for the reverse current, which was made smaller by up to 80%. This is shown at the bottom of figure 7.

The results in figure 8 (top and center) report the time dependence of forward bias voltage injection at 10 V. This forward current density was larger by almost a factor of 10 for carrier I njection for 1 h. This is roughly 50% of the reducton die to the initial damage induced by the irradtion with protons. The trend was that the reverse current density was reduced monotonically with injection time (figure 8, bottom) . By sharp contrast, the forward current density was found to tdegrade for long injection periods. This was also observed in previous studies [63]. It is important to point out that conventional thermal annealing ,ust be carried out at temperatures of at least 300 °C–400 °C in order to observe significant reduxtion in the damage for similar fluence and energies to the conditions eompluyed in this work [36]. The temperatuire of devices in our experiments did not rise above ~50 °C during carrier injection, so thermal damage is not present.

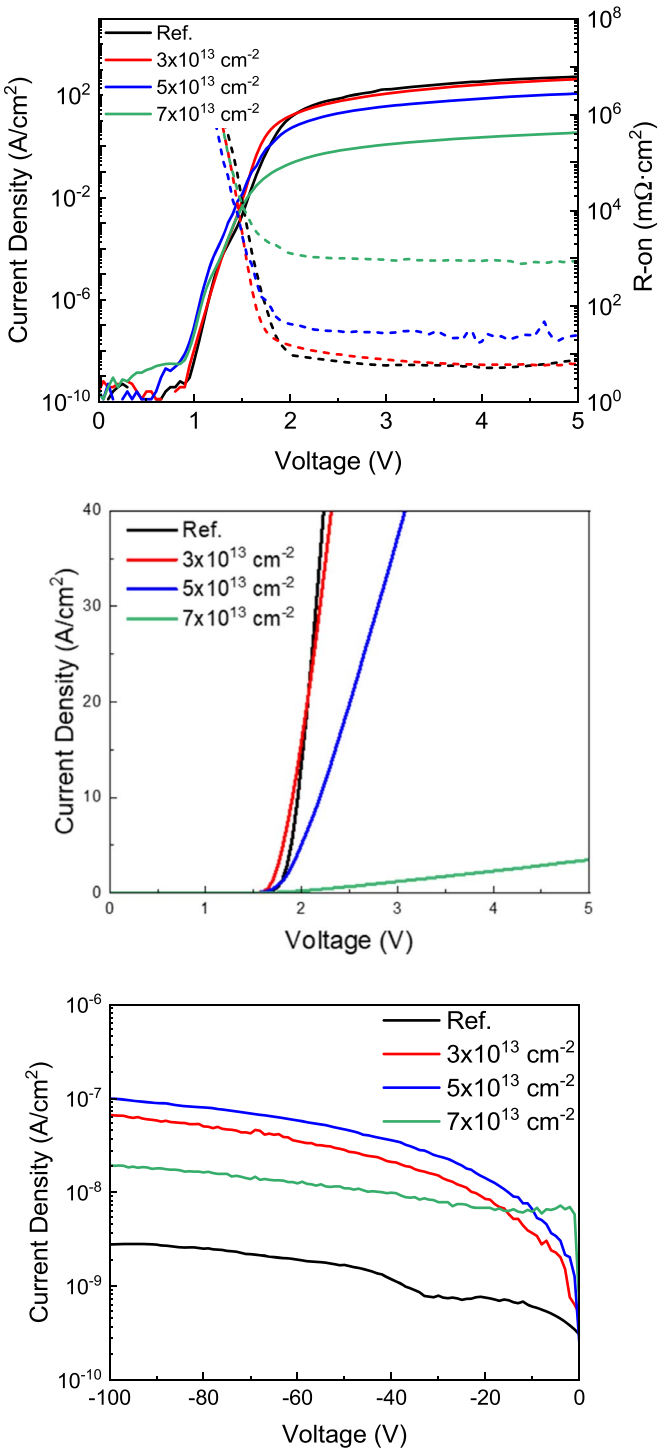

Figure 4. J-I characteristics as a function of H^+ fluence shown on log (top) or linear scale (center) and reverse current density in low voltage region before and after irradiation.

To understand the mechanism for improvement of the transport properties upon carrier I jection, it is important to note that the minority carrier diffusion lengths in unirradated Ga_2O_3 range from 350–400 nm. When subject to proton irradiation, these are effectively reduced by approximately one half their intial value [46]. This demonstrates the influence of point defect introduction on minority carrier transport; however it precludes this mechanism from mitigating damage throughout the thick drift layer of the rectifiers. C-V profiling on the partially recovered irradiated devices indicated there was a uniform increase in electron density after the carrier injection (figure 5). Since an increase would be expected only within a few minority carrier diffusion lengths of the contact if recombination-enhanced annealing were occurring, we propose that an alternative carrier-induced mechanism is present

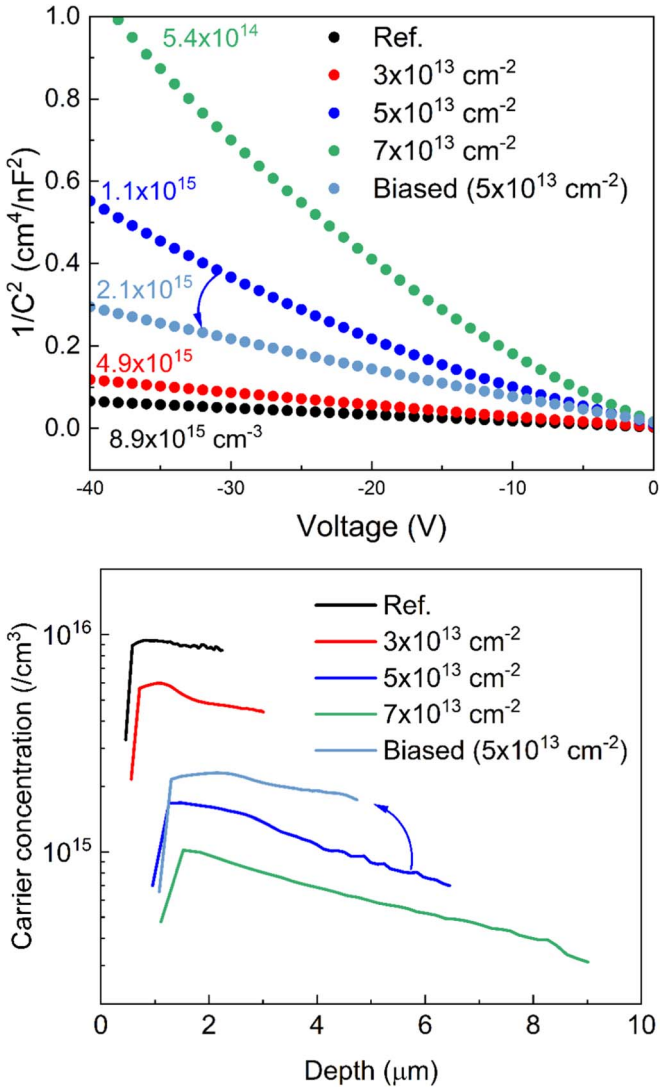

Figure 5. $1/C^2$-V characteristics as a function of H^+ fluence (top) and carrier depth profiles extracted this data (bottom).

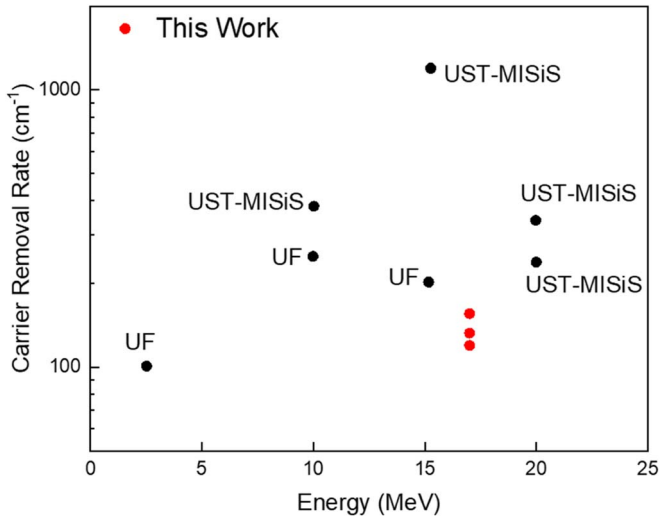

Figure 6. Carrier removal rates as a function of energy for protons in β-Ga_2O_3.

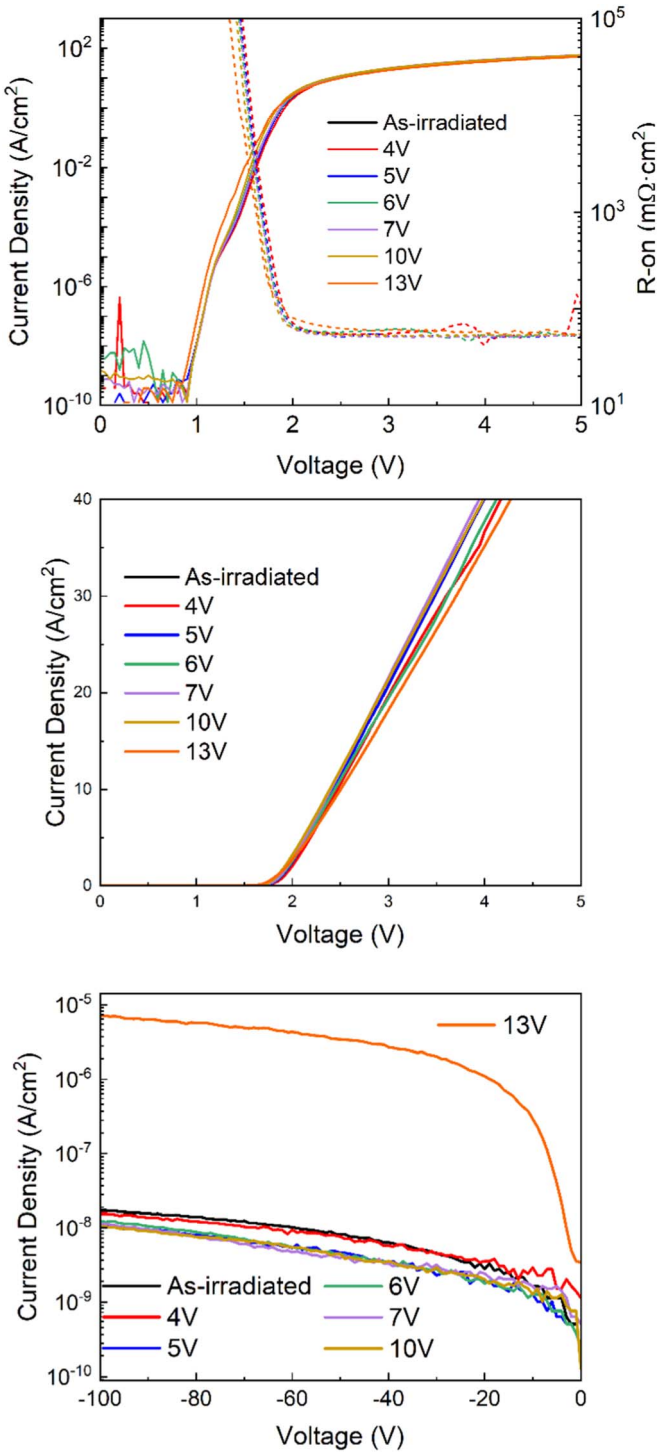

Figure 7. Forward (top/center) and reverse (bottom) J-I characteristics as a function of forward biasing at different bias voltages after irradiation with H^+ fluence of 5×10^{13} cm^{-2}.

During forward biasing, holes are injected from the p-type NiO, while electrons flow toward the top contact from the heavility doped substrate. This process is analgous to the EWF mechanism, wherein the momentum of the electrons facilitates defect annealing [49–60]. This mechanism is almost athermal, as evidenced by precise measurements of the device temperature during the application of pulsed currents at low duty cycles near room temperature [50]. Future work will focus on similar studies to examine changes in lattice strain and defect density in Ga_2O_3 rectifiers after pulsed current annealing cycles. Investigating the long-term stability will also be a priority.

Table 1 tabulates the relative changes in forward and reverse current densities, in addition to the changes in on-state resistance as a result of proton irradiation and subsequent thermal [36] or current injection annealing. Thermal annealing induces a significantly greater recovery of forward current and on-state resistance but

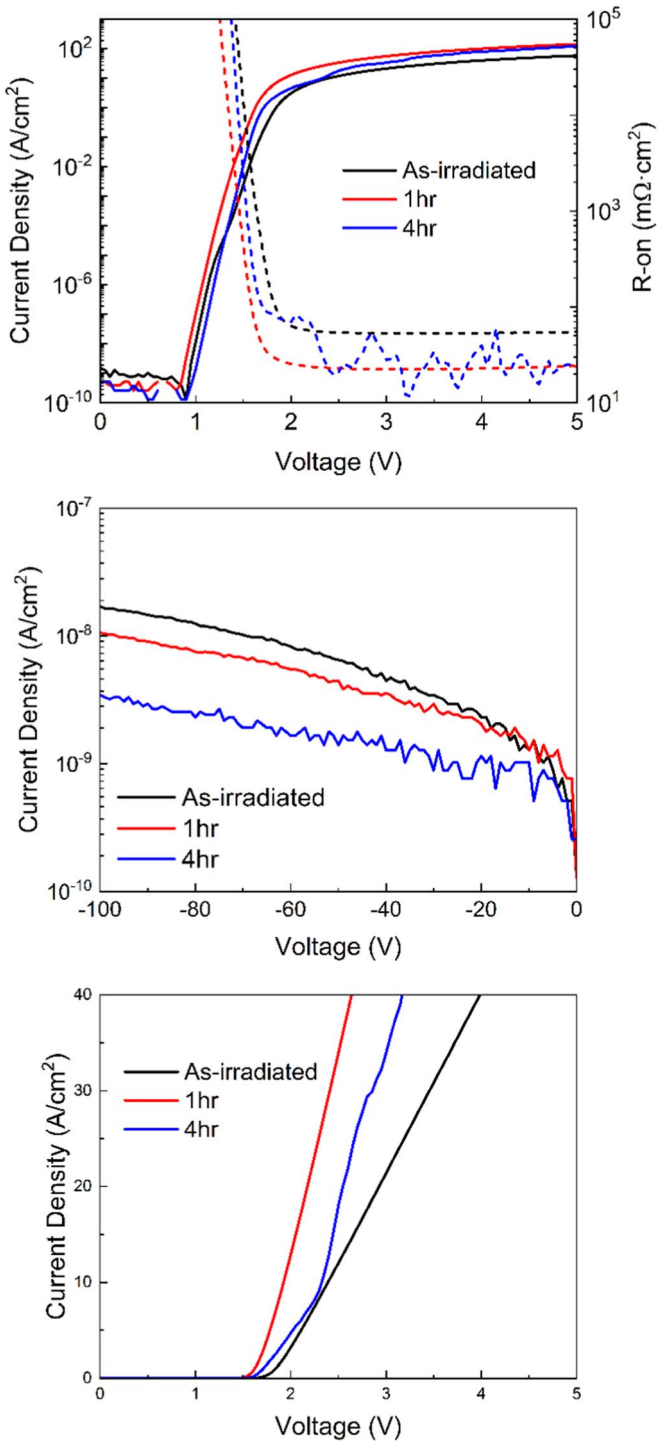

Figure 8. Forward (top/center) and reverse (bottom) J-I characteristics as a function of forward biasing at different bias durations after irradiation with H^+ fluence of 5×10^{13} cm^{-2}.

degrades the reverse current due to reactions between the metal contacts on the Ga_2O_3 rectifiers [36]. In contrast, the improvements observed with carrier injection are more modest, however this method does not cause thermal degradation of the device metallization.

Summary and conclusions

In synopsis, proton irradiation significantly impacts the performance of vertical geometry NiO/β-Ga_2O_3 heterojunction rectifiers, primarily manifesting as a decrease in forward current density, thereby elevating the RON of the devices. This effect stems from diminished carrier density and mobility within the drift layer. Concurrently, the reverse leakage current experiences an approximate twofold increase with higher fluence.

Table 1. Comparison of relative changes in select device parameters of proton irradiated NiO/Ga_2O_3 rectifiers as a result of subsequent thermal annealing at 400 °C or carrier injection near room temperature. I_F is the forward current density at 3 V bias, R_{ON} the on-state resistance and I_R the reverse current at 100 V.

Sample	I_F (3 V)	I_R (100 V)	R_{ON}
Proton irradiated (7–10 × 10^{13} cm^{-2})	↓100×	↑10×	↑100×
Thermal anneal 400 °C	↑10×	↑10×	↓10×
Carrier injection (10 V)	↑20%	↑5×	↓20%

The removal rates of carriers within the Ga_2O_3 layer range between 120 and 150 for the applied fluence range, akin to Schottky rectifiers lacking the NiO layer.

Following proton-induced damage, subsequent carrier injection experiments indicate partial recovery, discounting recombination-enhanced annealing due to the limited carrier diffusion length in Ga_2O_3. The predominant mechanism likely involves electron wind force annealing induced by momentum transfer from electronics to defect sites.However, there exists a threshold for injected charge beyond which benefits diminish. Under very heavy carrier injection conditions (forward bias of 13 V for 10 ks), the on-state current density decreases by 60%, while the reverse current density experiences a four-order-of-magnitude increase. This phenomenon is attributed to heightened interface states at the anode contact [63, 64].

Acknowledgments

The work at UF was performed as part of Interaction of Ionizing Radiation with Matter University Research Alliance (IIRM-URA), sponsored by the Department of the Defense, Defense Threat Reduction Agency under award HDTRA1-20-2-0002. The content of the information does not necessarily reflect the position or the policy of the federal government, and no official endorsement should be inferred. The work in Korea was supported by the Korea Institute for Advancement of Technology (KIAT) (P0012451, The Competency Development Program for Industry Specialist), the National Research Foundation of Korea (2020M3H4A3081799) and the K-Sensor Development Program (RS-2022-00154729), funded by the Ministry of Trade, Industry and Energy (MOTIE, Korea), the Institute of Civil Military Technology Cooperation Center funded by the Defense Acquisition Program Administration and Ministry of Trade, Industry and Energy, and of Korean government (20-CM-BR-05) and Korea Research Institute for defense Technology planning and advancement (KRIT) grant funded by Defense Acquisition Program Administration (DAPA) (KRIT-CT-21-034 and KRIT-CT-22-046). The work at PSU was also funded by the US National Science Foundation (ECCS # 2015795). The work at UCF was supported in part by the US-Israel Binational Science Foundation (award #2022056), the National Science Foundation (ECCS #2310285), and NATO (G-6072 and G-6194).

Data availability statement

The data cannot be made publicly available upon publication because no suitable repository exists for hosting data in this field of study. The data that support the findings of this study are available upon reasonable request from the authors.

Author declarations

The authors have no conflicts to disclose.

Data availability

The data that supports the findings of this study are available within the article.

Declarations

The authors have no conflicts to disclose.

ORCID iDs

Jian-Sian Li https://orcid.org/0000-0002-2817-7612
Hsiao-Hsuan Wan https://orcid.org/0000-0002-6986-8217
Aman Haque https://orcid.org/0000-0001-6535-5484
Jihyun Kim https://orcid.org/0000-0003-2367-8693
S J Pearton https://orcid.org/0000-0001-6498-1256

References

[1] Lu X, Deng Y X, Pei Y L, Chen Z M and Wang G 2023 Recent advances in NiO/Ga_2O_3 heterojunctions for power electronics *J. Semicond.* **44** 061802
[2] Green A J *et al* 2022 β-Gallium oxide power electronics *APL Mater.* **10** 029201
[3] Pearton S J, Ren F, Tadjer M and Kim J 2018 Perspective: Ga_2O_3 for ultra-high power rectifiers and MOSFETS *J. Appl. Phys.* **124** 220901
[4] Kalra A, Ul Muazzam U, Muralidharan R, Raghavan S and Nath D N 2022 The road ahead for ultrawide bandgap solar-blind UV photodetectors *J. Appl. Phys.* **131** 150901
[5] Sharma S, Zeng K, Saha S and Singisetti U 2020 Field-plated lateral Ga_2O_3 MOSFETs with polymer passivation and 8.03 kV breakdown voltage *IEEE Electron Dev. Lett* **41** 836
[6] Wang C, Zhang J, Xu S, Zhang C, Feng Q, Zhang Y, Ning J, Zhao S, Zhou H and Hao Y 2021 Progress in state-of-the-art technologies of Ga_2O_3 devices *Journal of Physics D: Appl. Phys.* **54** 243001
[7] Li J S, Chiang C C, Xia X, Wan H H, Ren F and Pearton S J 2023 7.5 kV, 6.2 GW cm^{-2} NiO/β-Ga_2O_3 vertical rectifiers with on–off ratio greater than 10^{13} *J. Vacuum Sci. Technol. A* **41** 030401
[8] Zho F *et al* 2023 An avalanche-and-surge robust ultrawide-bandgap heterojunction for power electronics *Nat. Commun.* **14** 4459
[9] Zhang J *et al* 2022 Ultrawide Bandgap Semiconductor Ga_2O_3 Power diodes *Nature Commun* **13** 3900
[10] Dong P, Zhang J, Yan Q, Liu Z, Ma P, Zhou H and Hao Y 2022 6 kV/3.4 mΩ·cm^2 Vertical β-Ga_2O_3 Schottky Barrier Diode With BV^2/Ron,sp performance exceeding 1D unipolar limit of GaN and SiC *IEEE Electron Dev Lett.* **43** 765
[11] Li J-S, Chiang C-C, Xia X, Jinsoo Yoo T, Ren F, Kim H and Pearton S J 2022 Demonstration of 4.7 kV breakdown voltage in NiO/β-Ga_2O_3 vertical rectifiers *Appl. Phys. Lett.* **121** 042105
[12] Liao C *et al* 2022 Optimization of NiO/β-Ga_2O_3 heterojunction diodes for high-power application *IEEE T Electron Dev* **69** 5722
[13] Xiao M *et al* 2021 Packaged Ga_2O_3 Schottky Rectifiers With Over 60-A Surge Current Capability *IEEE Trans. Power Electron.* **36** 8565
[14] Yan Q *et al* 2021 β-Ga_2O_3 hetero-junction barrier Schottky diode with reverse leakage current modulation and $BV^2/R_{on,sp}$ value of 0.93 GW/cm^2 *Appl. Phys. Lett.* **118** 122102
[15] Gong H H, Chen X H, Xu Y, Ren F-F, Gu S L and Ye J D 2020 A 1.86-kV double-layered NiO/β-Ga_2O_3 vertical p-n heterojunction diode *Appl. Phys. Lett.* **117** 022104
[16] Gong H H *et al* 2021 β-Ga_2O_3 vertical heterojunction barrier Schottky diodes terminated with p-NiO field limiting rings *Appl. Phys. Lett.* **118** 202102
[17] Hao W, He Q, Zhou K, Xu G, Xiong W, Zhou X, Jian G, Chen C, Zhao X and Long S 2021 Low defect density and small I − V curve hysteresis in NiO/β-Ga_2O_3 pn diode with a high PFOM of 0.65 GW/cm^2 *Appl. Phys. Lett.* **118** 043501
[18] Zhou F *et al* 2022 1.95-kV beveled-mesa NiO/β-Ga_2O_3 heterojunction diode with 98.5% conversion efficiency and over million-times overvoltage ruggedness, *IEEE T Power Electr* **37** 1223
[19] Yan Q, Gong H, Zhou H, Zhang J, Ye J, Liu Z, Wang C, Zheng X, Zhang R and Hao Y 2022 Low density of interface trap states and temperature dependence study of Ga_2O_3 Schottky barrier diode with p-NiOx termination *Appl. Phys. Lett.* **120** 092106
[20] Wang Y *et al* 2022 2.41 kV Vertical P-NiO/n-Ga_2O_3 Heterojunction Diodes With a Record Baliga's figure-of-Merit of 5.18 GW/cm^2, *IEEE T Power Electr.* **37** 3743
[21] Wang Z *et al* 2022 Majority and minority carrier traps in NiO/β-Ga_2O_3 p^+-n heterojunction diode *IEEE T Electron Dev* **69** 981
[22] Wang B, Xiao M, Spencer J, Qin Y, Sasaki K, Tadjer M J and Zhang Y 2023 2.5 kV vertical Ga_2O_3 schottky rectifier with graded junction termination extension *IEEE Electron Dev. Lett.* **44** 221
[23] Sian Li J, Ching Chiang C, Xia X, Hsuan Wan H, Ren F and Pearton S J 2023 Superior high temperature performance of 8 kV NiO/Ga_2O_3 vertical heterojunction rectifiers *J. Mater. Chem. C* **11** 7750
[24] Li J S, Wan H H, Chiang C C, Xia X, Yoo T, Kim H, Ren F and Pearton S J 2023 Reproducible NiO/ Ga_2O_3 vertical rectifiers with breakdown voltage > 8 kV *Crystals* **13** 886
[25] Li J S *et al* 2023 Effect of Drift Layer Doping and NiO parameters in achieving 8.9 kV breakdown in 100 μm diameter and 4 kV/4A in 1 mm diameter NiO/Ga_2O_3 rectifiers *J. Vac. Sci. Technol.* A **41** 043404
[26] Kim J *et al* 2019 Radiation damage effects in Ga_2O_3 materials and devices *J. Mater. Chem.* C **7** 10
[27] Xia X *et al* 2022 Radiation damage in the ultra-wide bandgap semiconductor Ga_2O_3 *ECS J. Solid State Sci. Technol.* **11** 095001
[28] Hoi Wong M, Takeyama A, Makino T, Ohshima T, Sasaki K, Kuramata A, Yamakoshi S and Higashiwaki M 2018 Radiation hardness of β-Ga_2O_3 metal-oxide-semiconductor field-effect transistors against gamma-ray irradiation *Appl. Phys. Lett.* **112** 023503
[29] Li J-S, Chiang C-C, Xia X, Stepanoff S, Haque A, Wolfe D E, Ren F and Pearton S J 2023 Reversible total ionizing dose effects in NiO/Ga_2O_3 heterojunction rectifiers *J. Appl. Phys* **133** 015702
[30] Tuttle B R, Karom N J, O'Hara A, Schrimpf R D and Pantelides S T 2023 Atomic-displacement threshold energies and defect generation in irradiated β-Ga_2O_3: a first-principles investigation *J. Appl. Phys.* **133** 015703
[31] Yakimov E B, Polyakov A Y, Shchemerov I V, Smirnov N B, Vasilev A A, Vergeles P S, Yakimov E E, Chernykh A V, Ren F and Pearton S J 2021 Experimental estimation of electron–hole pair creation energy in β-Ga_2O_3 *Appl. Phys. Lett.* **118** 202106
[32] Cadena R M *et al* 2023 Low-energy ion-induced single-event burnout in Ga_2O_3 schottky diodes *IEEE Trans Nuclear Sci.* **70** 363
[33] Ma H, Wang W, Cai Y, Wang Z, Zhang T, Feng Q, Chen Y, Zhang C, Zhang J and Hao Y 2023 Analysis of single event effects by heavy ion irradiation of Ga_2O_3 metal–oxide–semiconductor field-effect transistors *J. Appl. Phys.* **133** 085701
[34] Datta A and Singisetti U 2024 Simulation studies of single event effects in β-Ga_2O_3 MOSFETs *IEEE Trans. Nucl. Sci.* **71** 476
[35] Sharma R, Li J S, Law M E, Ren F and Pearton S J 2023 Effect of biased field rings to improve charge removal after heavy-ion strikes in vertical geometry β-Ga_2O_3 rectifiers *ECS J. Solid State Sci. Technol.* **12** 035003
[36] Li J-S, Chiang C-C, Xia X, Wan H-H, Kim J, Ren F and Pearton S J 2023 15 MeV proton damage in NiO/β-Ga_2O_3 vertical rectifiers, *J. Phys. Mater.* **6** 045003

[37] Maeda K 2013 Radiation-enhanced dislocation glide: the current state of research chapter 9 in ed O Ueda and S J Pearton *Materials and Reliability Handbook for Semiconductor Optical and Electron Devices* (Springer Science Business Media)
[38] Kimerling L C 1978 Recombination enhanced defect reactions *Solid State Electron.* **21** 1392
[39] Chernyak L, Nootz G and Osinsky A 2001 Enhancement of minority carrier transport in forward biased GaN p-n junction *Electron. Lett.* **37** 922
[40] Chernyak L, Osinsky A, Fuflyigin V and Schubert E F 2000 Electron beam-induced increase of electron diffusion length in p-type GaN and AlGaN/GaN superlattices *Appl. Phys. Lett.* **77** 875
[41] Chernyak L L, Burdett W, Klimov M and Osinsky A 2003 Cathodoluminescence studies of the electron injection induced effects in GaN *Appl. Phys. Lett.* **82** 3680
[42] Lopatiuk-Tirpak O, Chernyak L, Mandalapu L J, Yang Z, Liu J L, Gartsman K, Feldman Y and Dashevsky Z 2006 Influence of electron injection on the photoresponse of ZnO homojunction diodes *Appl. Phys. Lett.* **89** 142114
[43] Modak S, Chernyak L, Khodorov S, Lubomirsky I, Yang J, Ren F and Pearton S J 2019 Impact of electron injection and temperature on minority carrier transport in alpha-irradiated ß-Ga_2O_3 schottky rectifiers *ECS J. Solid State Sci. Technol.* **8** Q3050
[44] Modak S, Lee J, Chernyak L, Yang J, Ren F, Pearton S J, Khodorov S and Lubomirsky I 2019 Electron injection-induced effects in Si-doped β-Ga_2O_3 *AIP Adv.* **9** 015127
[45] Modak S, Chernyak L, Khodorov S, Lubomirsky I, Ruzin A, Xian M, Ren F and Pearton S J 2020 Effect of electron injection on minority carrier transport in 10 MeV proton irradiated β-Ga_2O_3 schottky rectifiers *ECS J. Solid State Sci. Technol.* **9** 045018
[46] Zhang Y and Weber W J 2020 Ion irradiation and modification: the role of coupled electronic and nuclear energy dissipation and subsequent nonequilibrium processes in materials *Appl. Phys. Rev.* **7** 041307
[47] Weber W J, Duffy D M, Thomé L and Zhang Y 2015 The role of electronic energy loss in ion beam modification of materials *Current Opinion Solid State Mater Sci* **19** 1–11
[48] Azarov A, Venkatachalapathy V, Lee I-H and Kuznetsov A 2023 Thermal versus radiation-assisted defect annealing in β-Ga_2O_3 *J. Vac. Sci. Technol. A* **41** 023101
[49] Rasel M A J, Stepanoff S, Haque A, Wolfe D E, Ren F and Pearton S 2022 Non-thermal annealing of gamma irradiated GaN HEMTs with electron wind force *ECS J. Solid State Sci. Technol.* **11** 075002
[50] Sultan Al-Mamun N, Gallagher J, Jacobs A G, Hobart K D, Anderson T J, Gunnin B P, Kaplar R J, Wolfe D E and Haque A 2024 Improving vertical GaN p–n diode performance with room temperature defect mitigation, *Semicond. Sci. Technol.* **39** 015004
[51] Sultan Al-Mamun N, Sheyfer D, Liu W, Haque A, Wolfe D E and Pagan D C 2024 Low temperature recovery of OFF-state stress induced degradation of AlGaN/GaN high electron mobility transistors *Appl. Phys. Lett.* **124** 013507
[52] Jafar Rasel M A, Sultan Al-Mamun N, Stepanoff S, Haque A, Wolfe D E, Ren F and Pearton S J 2023 Ultrafast, room temperature rejuvenation of SiC Schottky diodes from forward current-induced degradation *Appl. Phys. Lett.* **122** 204101
[53] Rasel M, Jafar A, Wyatt B, Wetherington M, Anasori B and Haque A 2021 Low-temperature annealing of 2D Ti3C2Tx MXene films using electron wind force in ambient conditions *J. Mater. Res.* **36** 3398
[54] Al-Mamun N S, Wolfe D E, Haque A, Yim J-G and Kim S K 2023 Room temperature annealing of SnS_2 films with electron impulse force *Scr. Mater.* **224** 115107
[55] Islam Z, Kozhakhmetov A, Robinson J and Haque A 2020 *J. Electron. Mater.* **49** 3770
[56] Ba X, Zhou M, Zhang X and Wang H 2020 Manipulating dislocations using electric field to repair embrittlement damage *ISIJ Int.* **60** 1803
[57] Xiang S and Zhang X 2019 Dislocation structure evolution under electroplastic effect *Mater. Sci. Eng. A* **761** 138026
[58] Zhu R, Jiang Y, Guan L, Li H and Tang G 2016 Difference in recrystallization between electropulsing-treated and furnace-treated NiTi alloy *J. Alloys Comp.* **658** 548
[59] Hu G, Zhu Y, Tang G, Shek C and Liu J 2011 Effect of electropulsing on recrystallization and mechanical properties of silicon steel strips *J. Materials Sci. Technol,* **27** 1034
[60] Kim M J, Lee K, Oh K H, Choi I-S, Yu H-H, Hong S-T and Han H N 2014 'Electric current-induced annealing during uniaxial tension of aluminum alloy, *Scr. Mater.* **75** 58
[61] Ziegler J F, Ziegler M D and Biersack J P 2010 SRIM—the stopping and range of ions in matter (2010) *Nucl. Instrum. Methods Phys. Res. B* **268** 1818
[62] Boschini M J, Rancoita P G and Tacconi M 2014 SR-NIEL- 7 calculator: screened relativistic (SR) treatment for calculating the displacement damage and nuclear stopping powers for electrons, protons *Light- and Heavy- Ions in Materials (version 9.3); [Online] Website Currently supporzted Within the Space Radiation Environment Activities of ASIF (ASI - Italian Space Agency -Supported Irradiation Facilities)* June 2023 http://Sr-niel.org/
[63] Gong S, Zheng X, Yue S, Hong Y, Zhang F, Wang Y, Wang X, Ma X, Xiaohua H and Hao Y Impact of high-temperature forward bias stress on the electrical performance degradation of β-Ga_2O_3 schottky barrier diodes *IEEE Trans. Electron Dev* in press
[64] Yakimov E B, Polyakov A Y, Smirnov N B, Shchemerov I V, Yang J, Ren F, Yang G, Kim J and Pearton S J 2018 Diffusion length of non-equilibrium minority charge carriers in β-Ga_2O_3 measured by electron beam induced current *J. Appl. Phys.* **123** 185704